



A large scale high-throughput screen identifies chemical inhibitors of phosphatidylinositol 4-kinase type II alpha^S

Nivedita Sengupta,* Marko Jović,* Elena Barnaeva,[†] David W. Kim,[†] Xin Hu,[†] Noel Southall,[†] Milan Dejmek,[§] Ivana Mejdrova,[§] Radim Nencka,[§] Adriana Baumlova,[§] Dominika Chalupska,[§] Evzen Boura,[§] Marc Ferrer,[†] Juan Marugan,[†] and Tamas Balla^{1,*}

Section on Molecular Signal Transduction,* Program for Developmental Neuroscience, Eunice Kennedy Shriver National Institute of Child Health and Human Development, National Institutes of Health, Bethesda, MD 20892; Division of Preclinical Innovation,[†] National Center for Advancing Translational Sciences, Rockville, MD 20850; and Institute of Organic Chemistry and Biochemistry,[§] Academy of Sciences of the Czech Republic, 166 10 Prague 6, Czech Republic

ORCID IDs: 0000-0002-0310-7730 (M.J.); 0000-0002-9077-3335 (T.B.)

Abstract The minor phospholipid, phosphatidylinositol 4-phosphate (PI4P), is emerging as a key regulator of lipid transfer in ER-membrane contact sites. Four different phosphatidylinositol 4-kinase (PI4K) enzymes generate PI4P in different membrane compartments supporting distinct cellular processes, many of which are crucial for the maintenance of cellular integrity but also hijacked by intracellular pathogens. While type III PI4Ks have been targeted by small molecular inhibitors, thus helping decipher their importance in cellular physiology, no inhibitors are available for the type II PI4Ks, which hinders investigations into their cellular functions. Here, we describe the identification of small molecular inhibitors of PI4K type II alpha (PI4K2A) by implementing a large scale small molecule high-throughput screening. A novel assay was developed that allows testing of selected inhibitors against PI4K2A in intact cells using a bioluminescence resonance energy transfer approach adapted to plate readers. The compounds disclosed here will pave the way to the optimization of PI4K2A inhibitors that can be used in cellular and animal studies to better understand the role of this enzyme in both normal and pathological states.—Sengupta, N., M. Jović, E. Barnaeva, D. W. Kim, X. Hu, N. Southall, M. Dejmek, I. Mejdrova, R. Nencka, A. Baumlova, D. Chalupska, E. Boura, M. Ferrer, J. Marugan, and T. Balla. **A large scale high-throughput screen identifies chemical inhibitors of phosphatidylinositol 4-kinase type II alpha.** *J. Lipid Res.* 2019. 60: 683–693.

Supplementary key words phosphoinositide • endosome • vesicular traffic

This work was supported in part by the intramural research programs of the Eunice Kennedy Shriver National Institute of Child Health and Human Development at the National Institutes of Health and the National Center for Advancing Translational Studies under the 1X01MH099804 grant. The work of M.D., I.M., R.N., A.B., D.C. and E.B. was supported by European Regional Development Fund Grant CZ.02.1.01/0.0/0.0/16_019/0000729 [Operational Programme Research, Development and Education (OP RDE) Project: “Chemical biology for drugging undruggable targets (ChemBioDrug)”].

Manuscript received 3 October 2018 and in revised form 8 January 2019.

Published, *JLR Papers in Press*, January 9, 2019
DOI <https://doi.org/10.1194/jlr.D090159>

Phosphoinositides represent a small fraction of all phospholipids, but they regulate a whole range of cellular processes (1). These regulatory lipids are formed by sequential phosphorylation of phosphatidylinositol (PI) on its inositol ring at any of three positions (positions 3, 4, and 5). The different combination of these phosphorylations gives rise to the seven known PI species. There are specific enzymes for phosphorylation of each position and in most cases multiple enzymes catalyze the same reaction. A similar multiplicity of phosphatases exists, setting up an elaborate network of PI metabolism (1). Many of these enzymes have been linked to deregulation of PIP levels and human diseases. For example, numerous studies have investigated the role of PI3Ks and their lipid product, PI(3,4,5)P₃, in cancer and immune regulations promoting the development of PI3K inhibitors currently in clinical trials (2). PI 4-kinases (PI4Ks) phosphorylate the 4-position on the ring and have long been viewed only as enzymes that produce an intermediate for the synthesis of PI(4,5)P₂, a plasma membrane (PM) lipid of great significance (1, 3). However, research in the last 10 years revealed that the four distinct PI4Ks make PI 4-phosphate (PI4P) in various intracellular compartments, such as the Golgi and endosomes, where the lipid regulates trafficking of various cargos (3). There is now a better understanding of the cellular functions and importance of type III PI4Ks: PI4KB plays a role in the organization of the Golgi and trafficking through this compartment

Abbreviations: BRET, bioluminescence resonance energy transfer; HCV, hepatitis C virus; HTS, high-throughput screening; PI, phosphatidylinositol; PI4K, phosphatidylinositol 4-kinase; PI4K2A, phosphatidylinositol 4-kinase type II alpha; PM, plasma membrane; PI4P, phosphatidylinositol 4-phosphate; qHTS, quantitative high-throughput screening.

¹To whom correspondence should be addressed.

e-mail: ballat@mail.nih.gov

^SThe online version of this article (available at <http://www.jlr.org>) contains a supplement.

(4); whereas, PI4KA has functions at the ER and the PM at junctional sites where the two kinds of membranes are juxtaposed (5). Much less is known about the type II PI4Ks [PI4K type II alpha (PI4K2A) and PI4K2B] that are present in endomembranes, including the *trans*-Golgi network, and they have been shown to contribute to the regulation of trafficking through various endocytic compartments (6).

The relevance of PI4Ks has largely increased lately after the discovery that hepatitis C virus (HCV) replication requires the host PI4KA enzyme, whereas several enteropathogenic viruses utilize PI4KB for their replication (7). Based on these discoveries, several pharmaceutical companies are developing inhibitors that target the type III PI4Ks. These efforts have been greatly aided by the fact that type III PI4Ks are structural relatives of PI3Ks, and isoform-specific PI3K inhibitors have already been pursued for treatment of cancer and various inflammatory conditions (8). Interestingly, several drugs that have been in the pipeline to inhibit HCV (9) or enteroviruses (10) without solid knowledge of their mechanism of action turned out to inhibit the type III PI4Ks. It is also notable that various HCV strains vary in their PI4K needs; some use exclusively PI4KA, whereas some others use PI4KB and some enteroviruses already show resistance to drugs that we now know inhibit type III PI4Ks of the host cell (10, 11). These observations suggest that viruses can adapt to utilizing different PI4Ks to generate their replication platform, and mutations will allow them to switch enzymes under selection pressure. Because type II PI4Ks belong to a different family of enzymes with no close relatives within the kinase network, they are not targeted by any of the type III PI4K or PI3K inhibitors (12). Because of their localization and functional properties, these enzymes assume some overlapping functions with the type III PI4Ks, especially PI4KB, and will be available for viruses that need PI4P when type III enzymes are inhibited. Modulators of the type II enzymes would provide a better understanding of their physiological functions and their involvement in human disease, and it might trigger an interest in them as targets for development of therapeutics.

Independently, type II PI4Ks, but not the type III enzymes, were found to be needed for Wnt signaling (13–15). It is not clear how the enzyme contributes to the Wnt signaling cascade. Some studies suggested that PI(4,5)P₂ at the PM is important for Wnt signaling (13–15), but our research showed no effect of type II PI4K knockdown on PM PI(4,5)P₂ levels (12). However, in recent studies, we identified LRP10 as an interacting protein of PI4K2A (16). LRP10 is a transmembrane protein that is a negative regulator of Wnt signaling, inhibiting signaling from the LRP6/Fz receptor complex (17). LRP10 cycles between the PM and recycling compartments (our unpublished observation). The LRP6/Fz complex also undergoes endocytosis, and it is speculated that it signals from endocytic compartments (18). Given the role of PI4K2A in the endocytic network, its role in Wnt signaling could be related to the endocytic processing of the Wnt signaling complex. This raises the possibility that, regardless of its mode of action, targeting PI4K2A [and PI4K2B, as the two enzymes are almost indistinguishable catalytically (19)] could be an effective way of

inhibiting Wnt signaling. Wnt signaling is critical in early development, but, as many other developmentally important signaling cascades, it reactivates and drives certain types of cancer cells (20). In particular, together with K-Ras mutations, Wnt signaling was found to be a determinant for lineage selection in pancreatic ductal adenocarcinoma (21, 22). Wnt signaling was also found to be critical in the bone lesions developing in multiple myeloma (23, 24). Targeting Wnt signaling, therefore, is a priority for several pharmaceutical companies (20, 25) (see also <http://pharmastrategyblog.com/2010/09/wnt-signaling-and-cancer.html/>).

Other cellular processes that have been linked to type II PI4Ks include Akt activation and cancer cell growth (26), an effect that can also be related to the signaling features of Akt in endosomes (27–29) and the role of PI4K2A in endocytic trafficking. Our recent studies suggest that PI4K2A has an important role in the delivery of the GBA enzyme (an enzyme whose defective lysosomal activity is the cause of Gaucher disease) to the lysosome (30). Therefore, both positive and negative manipulations of the PI4K2A enzyme hold significant promise in understanding and possibly treating a whole range of lysosomal disorders.

Finally, the most recent research unveiled an important role of intermembrane gradients of PI4P, the lipid product of PI4Ks, as a source of energy to drive nonvesicular lipid transport between adjacent membranes in organelle contact sites (31). Several lipid transport proteins were found to bind PI4P as one of their cargoes, and, depending on the organelles involved, the PI4P is provided by distinct PI4K enzymes. This placed PI4Ks in the center of lipid metabolism, and, hence, membrane biogenesis and studies are emerging that suggest that defects in these lipid transport processes may have close links to neurodegenerative diseases, such as ALS (32), Parkinson (33), or demyelinating neuropathies (34).

Based on all of these data linking type II PI4Ks to many physiological processes relevant to a variety of diseases, it would be desirable to find inhibitors for PI4K2A, the class of PI4Ks for which inhibitors are not available as yet. A recent study described an inhibitor (PI-273) of PI4K2A (35), which showed promise in inhibiting cancer cell growth. That study used docking-based and ligand-based screening strategy to identify PI-273, which was found to interfere with substrate binding or substrate access and not with ATP binding (35). Our studies have used a different strategy, namely, the screening of a small molecule library of compounds using a recombinant PI4K2A. The inhibitors identified in our study have a different mode of action, interfering with ATP binding rather than with the binding of the lipid substrate.

MATERIALS AND METHODS

DNA constructs

PI4K2A-mRFP-N1 plasmid. PI4K2A-mRFP was made by exchanging the GFP to mRFP in the previously described PI4K2A-GFP construct (36). The endosomal PI4P bioluminescence resonance

energy transfer (BRET) probe was designed to express a Rab7-directed Venus together with an S-luciferase-fused PI4P reporter from a single plasmid such that PI4P made on endosomes would excite the endosome-targeted Venus via bioluminescence energy transfer. For this, a pmRFP-C1-Sluciferase-P4M2X-T2A-Venus-Rab7 plasmid was created in multiple steps. First, a Venus-Rab7 construct was made using the iRFP-FRB-Rab7 [described in (37)] by replacing the iRFP-FRB part of this construct with Venus (pmVenus-C1) using the *NheI*-*HindIII* fragments of the two plasmids. In the second step, the Sluciferase-P4M2x-T2 sequence was created by PCR using a forward primer containing a *NheI* site and a reverse primer containing the T2A sequence and an *AgeI* site. The L10-Venus-T2A-Sluciferase-P4M-2x plasmid was used as template after removing an internal *NheI* site from this original construct [described in (38)]. The PCR fragment was cloned into TOPO vector and the *NheI*-*AgeI*-digested insert was placed in the mVenus-Rab7 plasmid digested with *NheI*-*AgeI* to get the final construct.

Cell culture and transfection

The HEK293-AT1 cell line stably expressing the rat AT1a angiotensin receptor was described previously (12). The cell line was regularly tested for *Mycoplasma* contamination using InvivoGen mycoplasma detection kit each time after thawing and treated with Plasmocin prophylactic (InvivoGen) at 500 $\mu\text{g}/\text{ml}$ for 1 week. The subsequent passages were maintained at 5 $\mu\text{g}/\text{ml}$ of Plasmocin. HEK293-AT1 cells were cultured in DMEM (high glucose) containing 10% (v/v) FBS, 100 $\mu\text{g}/\text{ml}$ penicillin, and 100 $\mu\text{g}/\text{ml}$ streptomycin. COS-7 cells (also tested for *Mycoplasma*) were cultivated in DMEM containing 10% FBS, 100 $\mu\text{g}/\text{ml}$ penicillin, and 100 $\mu\text{g}/\text{ml}$ streptomycin. For confocal microscopy, COS-7 cells (200,000 cells/dish in 2 ml) were seeded onto glass-bottom dishes (30 mm diameter), transfected, and subjected to confocal microscopy. For BRET measurements, HEK-AT1 cells (50,000 cells/well in 200 μl , in triplicate) were plated onto white 96-well plates that were precoated with PLL, transfected, and subjected to BRET analysis. For immunoprecipitation of PI4K2A-mRFP, COS-7 cells (2,000,000 cells/dish in 10 ml) were seeded in 10 cm cell culture Petri dishes. Both HEK-AT1 and COS-7 cells were transfected with Lipofectamine 2000 transfection reagent (Thermo Fisher Scientific). For confocal microscopy, cells were transfected with DNA (0.1 μg DNA each) using Lipofectamine transfection reagent based on the manufacturer's standard protocol. For BRET measurements and in situ PI4K2A assay, cells were transfected with 0.1 μg DNA each well.

Purification of PI4K2A from *Escherichia coli*

The recombinant PI4K2A was expressed and purified as described previously (39) with minor modifications because of the large quantities of the recombinant enzyme needed. Briefly, PI4K2A was expressed in 100 liters of autoinduction medium with N-terminal 6xHis purification tag and GB1 solubilization tag followed by TEV protease cleavage site in *E. coli* BL21 NiCo strain. The bacteria were lysed in lysis buffer [50 mM Tris (pH 8), 300 mM NaCl, 3 mM β -ME, 20 mM imidazole, 10% glycerol] using EmulsiFlex (Avestin) and the protein was purified using affinity purification on Protino Ni-NTA agarose (Machery-Nagel), eluted using lysis buffer supplemented with 300 mM imidazole. The tag was cleaved by TEV protease and the protein was further purified using anion-exchange chromatography on a mono-Q column (GE Healthcare). Finally, the recombinant PI4K2A was concentrated to 7 mg/ml, aliquoted, and stored in -80°C until needed.

Purification of PI4K2A-mRFP from COS-7 cells

For purifying palmitoylated PI4K2A enzyme for kinase assay, COS-7 cells were transiently transfected with PI4K2A-mRFP

construct and protein was expressed for 2 days. Cells were harvested by washing once with 5 ml of PBS on ice and resuspended in 1 ml of ice-cold RIPA lysis buffer [50 mM Tris (pH 7.4), 150 mM NaCl, 1 mM EDTA, 0.25% deoxycholate, 1% Nonidet P-40, 1 mM Na_3VO_4 , 1 mM dithiothreitol, 10 $\mu\text{g}/\text{ml}$ aprotinin, and 10 $\mu\text{g}/\text{ml}$ leupeptin]. Cells were scraped, transferred into 2 ml microfuge tubes, and incubated on ice for 10 min for lysis. Cell lysates were centrifuged at 4°C , 15,000 g for 10 min to get rid of debris. The supernatant was collected in a separate 2 ml microfuge tube and incubated overnight at 4°C with 30 μl of pre-washed (three times in RIPA buffer) streptavidin-conjugated Dynabeads (Life Technologies, Carlsbad, CA) and 2 μl of biotin-conjugated anti-mRFP antibody (Rockland, Gilbertsville, PA) on a rotisserie rotor. The PI4K2A-mRFP-bound Dynabeads were collected by magnetic separation followed by washing five times with cold RIPA lysis buffer supplemented with 1 M LiCl and fresh protease inhibitors. Before using the PI4K2A-bound beads for kinase assay, they were washed three times in the kinase assay buffer [40 mM Tris-HCl (pH 7.5), 20 mM MgCl_2 , 1 mM EGTA (pH 7.5), 0.2% Triton X-100, 0.5 mM dithiothreitol, 0.1% BSA] before finally resuspending 200 μl of kinase assay buffer.

Miniaturized ADP-Glo assay for HTS

For the robotic screening, the ADP-Glo assay using the ADP-Glo™ kinase assay kit from Promega was miniaturized and optimized on 1,536-well white solid bottom plates (Greiner Bio-one). The substrate, 1.2 mM PI, prepared in the assay buffer [40 mM Tris (pH 7.5), 20 mM MgCl_2 , 1 mM EGTA, 0.4% Triton X-100, 0.5 mM DTT, 0.5 mg/ml BSA] and PI4K2A enzyme, diluted also in the assay buffer to 4 $\mu\text{g}/\text{ml}$, were dispensed onto the plates in equal volumes (1 $\mu\text{l}/\text{well}$), pinned with 23 nL/well tested compounds or control followed by dispensation of 1 $\mu\text{l}/\text{well}$ 300 μM ATP. The plates were incubated for 1 h. Then, 2 $\mu\text{l}/\text{well}$ of ADP-Glo reagent were added and incubated for 40 min. Next, 4 $\mu\text{l}/\text{well}$ of kinase detection buffer were added to the plates and incubated for an additional 40 min. All incubation steps were performed at ambient temperature. The resulting luminescence signal was measured on a Viewlux plate reader (PerkinElmer). Adenosine, a partial nonspecific inhibitor, was used as a positive control at 100 μM final concentration to assess the assay's quality and plate-to-plate reproducibility. We also used "no enzyme" control to gauge the assay's maximal potential inhibition (IC_{100}).

ADP-Glo assay for testing selected compounds

The ADP-Glo assay was performed using the ADP-Glo™ kinase assay kit from Promega with slight modifications in the total reaction volumes. The enzyme assay for the COS-7-expressed immunoprecipitated PI4K2A enzyme was done in a total volume of 200 μl . PI4K2A-bound Dynabeads (25 μl) suspended in kinase assay buffer were transferred in per well of a 96-well white plate and preincubated with 1 μl of inhibitor candidates (final concentration, 10 μM) at room temperature for 10 min. Following preincubation with inhibitors, 25 μl of kinase assay buffer containing 0.6 mM ultrapure ATP and 1.6 mM PI were added in each well and the reaction was continued at room temperature for 1.5 h. The reaction was stopped by adding 50 μl of ADP-Glo reagent, and further incubated for 40 min followed by addition of 100 μl of kinase detection reagent and incubation for 40 min in the dark at room temperature. The luminescence was measured using a Tristar2 LB 942 multimode microplate reader (Berthold Technologies).

In situ PI4K2A kinase assay with COS-7 cells

For determining the extent of inhibition on PI4K2A exerted by the candidate inhibitors in COS-7 cells, PI4K2A-mRFP was transfected to COS-7 cells and protein was expressed overnight. The transfected cells were incubated in 1 ml of modified Krebs-Ringer

buffer [120 mM NaCl, 4.7 mM KCl, 0.7 mM MgSO₄, 10 mM HEPES (pH 7.3), 1.802 g D+ glucose, 2 mM CaCl₂, with a final pH adjusted to 7.4] with 1 μM of PI4K2A inhibitors in a 37°C water bath for 20 min. After 20 min, 10 μM of wortmannin was added to each well following reincubation at 37°C for another 10 min. The medium was replaced with 500 μl of permeabilization buffer [110 mM KCl, 10 mM NaCl, 5 mM MgCl₂, 20 mM HEPES (pH 7.3), 2 mM EGTA, 0.05% BSA (v/v)] containing 15 μg/ml of digitonin, 0.3 mM freshly prepared ATP, 1 μM inhibitors, 10 μM of wortmannin, and 15 μl of 10 μCi/ml of P³²-labeled ATP. The cells were incubated in a 37°C water bath for 30 min. The reaction was stopped by quickly replacing the permeabilization buffer with 500 μl of ice chilled 1× PBS containing 5% perchloric acid followed by incubation on ice for 30 min. Cells were scraped and transferred to Eppendorf tubes, which were centrifuged at 16,000 g for 5 min at room temperature. The supernatant was discarded, and the pellet was resuspended in 800 μl of 1 N HCl and transferred to 15 ml polypropylene tubes. The phospholipids were extracted following the lipid extraction protocol (40).

BRET assay

For measuring the dynamic change of the endosomal PI4P level, vector (Sluc-P4M2X-T2A-Venus-Rab7)-transfected cells were subjected to BRET measurement. After 24 h of transfection, HEK-AT1 cells were rinsed once with modified Krebs-Ringer buffer [120 mM NaCl, 4.7 mM KCl, 0.7 mM MgSO₄, 10 mM HEPES (pH 7.3), 1.802 g D+ glucose, 2 mM CaCl₂, with a final pH adjusted to 7.4]. Cells were preincubated in 50 μl/well Krebs-Ringer buffer for 1 h at room temperature. Subsequent BRET measurements were done at room temperature. The cells were first subjected to a baseline measurement for 4 min (1 min/cycle) with 40 μl of luciferase substrate coelenterazine h added per well followed by addition of 10 μl/well Krebs-Ringer buffer containing DMSO or candidate inhibitors (final concentration 30 or 10 μM), and BRET measurement was conducted for 10 min. After 10 min, 10 μl of Krebs-Ringer buffer containing DMSO or A1 (final concentration 10 nM) were added per well, and BRET measurements were continued for additional time as indicated (1 min/cycle). In experiments requiring pretreatment with A1, following baseline measurements for 4 min, further measurement was conducted initially with A1 for 30 min and then with inhibitors mixed in 10 μl of Krebs-Ringer buffer for another 30 min (1 min/cycle). For BRET analysis of endosomal PI4P levels, BRET values were

calculated from measurements after adding coelenterazine h. A TriStar2 LB 942 multimode microplate reader (Berthold Technologies) equipped with 540/40 nm (Venus fluorescent measurement) and 475/20 nm (luciferase measurement) emission filters was used for BRET. Because of the robustness and reproducibility of this assay, testing the individual compounds for screening purposes was done in a single experiment, but the NC03 compound was always included as a positive control. Assays for compounds that showed inhibition were repeated one more time to confirm their activity.

Molecular docking studies

Crystal structure of PI4K2A was retrieved from the Protein Data Bank (4HNE). Docking of small molecule inhibitors to the active site of protein was performed using the MOE dock program (https://www.chemcomp.com/MOE-Structure_Based_Design.htm). The ligand-induced fit protocol was applied and the binding affinity was evaluated using the GBVI/WSA score. The best binding model with the lowest binding free energies was further energetically minimized using the MOE program. The PyMOL program was used to make the final graphs.

RESULTS

High-throughput screening for the discovery of small molecule PI4K2A inhibitors using a PI4K2A activity assay

The ADP-Glo assay described earlier by the Tai laboratory (41) was used as a starting point to develop a miniaturized version for high-throughput screening (HTS) applications. To implement the HTS screen, the PI4K ADP-Glo™ kinase assay (Promega, V9102) was miniaturized to a 1,536-well format to enable a large scale dose response quantitative HTS (qHTS) using an automated robotics platform. For the optimization of the assay, reagent concentrations, addition volumes, and reaction/incubation times were modified to obtain a Z-factor of >0.5 (see Fig. 1). The optimized 1,536-well plate assay protocol is shown in Table 1. Following establishment of 1,536 assay conditions, the qHTS assay was further validated by screening the LOPAC®1280 (Sigma-Aldrich) collection of biologically active compounds.

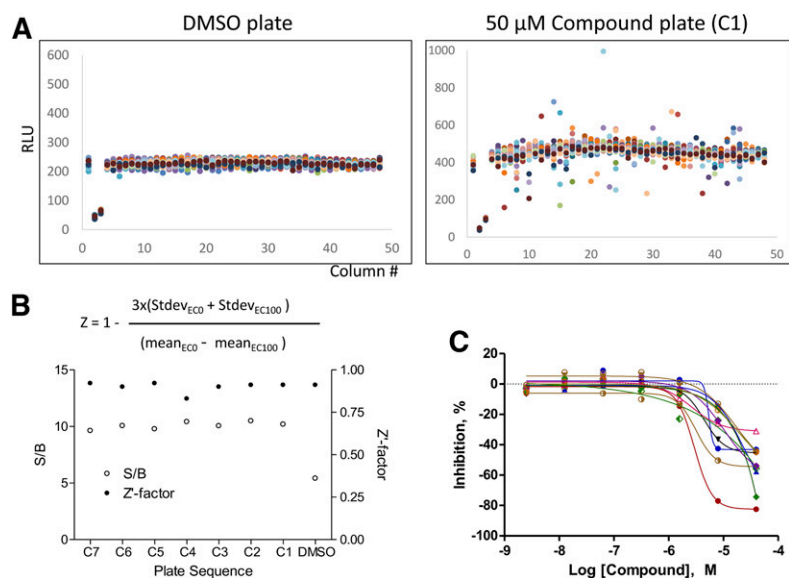


Fig. 1. Summary of LOPAC collection validation screening with the recombinant PI4K2A enzyme produced in bacteria using ADP-Glo assay. A: Scatter plots of plates treated with either DMSO (left) or compounds at the highest dose (50 μM) (right) on one single 1,536-well plate. Each plate contains 48 columns (x axis), each column contains 32 wells. Different compounds were added to each well in columns 5–48 as a single point at a single concentration. The seven concentrations of the drugs were tested in plates C1–C7. The controls were added onto columns 1–4 as follows: columns 1 and 4, DMSO (EC0); column 2, no enzyme (EC100); and column 3, adenosine at 100 μM. B: In each of the plates, including those where columns 5–48 were treated with inhibitors, the DMSO (EC0) and no enzyme (EC100) values were used to calculate the signal to background (S/B) ratios (open circles) and calculate the Z-factor (closed circles). C: Dose response curves of selected robust inhibitors.

TABLE 1. PI4K ADP-Glo™ kinase HTS protocol, 1,536-well format

Step	Parameter	Value	Description
1	Reagent	1 μ l	Substrate: 1.2 mM PI (400 μ M final)
2	Reagent	1 μ l	Enzyme: 4 μ g/ml PI4k2- α (as 3x)
3a	Compounds	23 nl	From screening libraries, 76 and 15 μ M final
3b	Intraplate control	23 nl	Partial inhibitor (adenosine, 100 μ M final)
4	Reagent	1 μ l	ATP (100 μ M final)
5	Time	1 h	Incubation (ambient temperature)
6	Reagent	2 μ l	ADP-Glo™ reagent, diluted 1:5 in assay buffer
7	Time	40 min	Incubation (ambient temperature)
8	Reagent	4 μ l	Kinase detection buffer, diluted 1:5 in assay buffer
9	Time	40 min	Incubation (ambient temperature)
10	Detection	Luminescence read, 1 s	ViewLux (PerkinElmer)

Seven concentrations of each compound were assayed from 4.8 nM to 76 μ M, with 5-fold dilutions (plates C1–C7, each containing a single concentration of the inhibitors). One assay plate with plain DMSO was used to determine the assay robustness in the absence of compounds (Fig. 1A). A total of eight assay plates were tested in the LOPAC pilot screen and the median assay parameters per plate were 10-fold signal-to-background ratio and the median Z' -factor was 0.85 calculated from the DMSO (EC0) and no enzyme (EC100) columns in each plate (Fig. 1B), thus further validating the reliability of this assay in 1,536-well format. Figure 1A shows scatter plots for two assay plates from the LOPAC screen, one testing a plate with DMSO and another with the highest dose of LOPAC compounds (single measurement for each compound). Using the curve class classification algorithms developed at the National Center for Advancing Translational Sciences Chemical Genomics Center for hit selection from dose response HTS (42), 17 compounds were determined to be high quality inhibitors of the PI4K ADP-Glo assay (\sim 1% hit rate). The assay was also able to detect 11 compounds as potential activators of PI4K2A (not shown).

A HTS identifies PI4K2A inhibitor candidates

A HTS was then performed with \sim 400,000 compounds from small molecule diversity collections. Sytravon, NPC, and MLPCN collections were screened at the top two doses (76 and 15 μ M final concentration) using a bacterially expressed human PI4K2A enzyme (39). Based on the screening

results, we identified \sim 580 compounds with $>$ 50% inhibitory activity. These compounds were retested at seven doses in 1:3 serial dilution to confirm their activity. Further, they were counter-screened with ADP-Glo™ reagents in the absence of the enzyme to exclude artificially luminescent compounds, and with PI4KB, another structurally unrelated PI4K. The list was further narrowed by eliminating compounds that were known inhibitors of protein kinases or were deemed structurally unsuitable for further development, yielding 14 inhibitors shortlisted for further studies. The workflow of HTS and confirmation is shown in Fig. 2. The structures of confirmed hits are shown in Fig. 3.

PI4K2A inhibitors also inhibit the mammalian expressed palmitoylated enzyme

The kinase activity of the human PI4K2A is largely increased when a cysteine-rich sequence (174-CCPCC-178) within the kinase domain is palmitoylated in the vertebrate enzyme providing strong membrane association (44). The palmitoylation was absent in the bacterially expressed enzyme used for the high-throughput screen, as the *E. coli* lacks the necessary enzyme needed for palmitoylation. Hence, we tested all of the 14 candidates using a human PI4K2A expressed and isolated from COS-7 cells. [In earlier studies, we showed palmitoylation of the expressed GFP-fused enzyme (45).] For this, PI4K2A-mRFP was expressed in COS-7 cells and immunoprecipitated in a two-step pull down assay using a biotin-conjugated anti-mRFP antibody along with anti-streptavidin-conjugated Dynabeads.

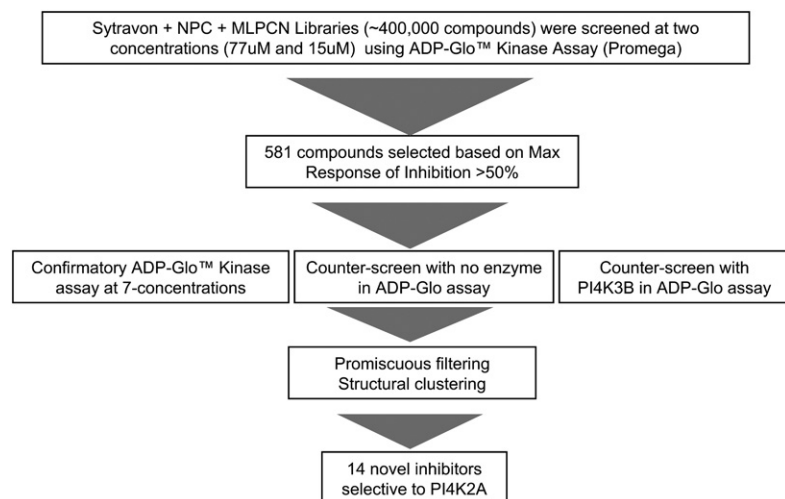


Fig. 2. Workflow of qHTS and hit validation for identification of PI4K2A inhibitors.

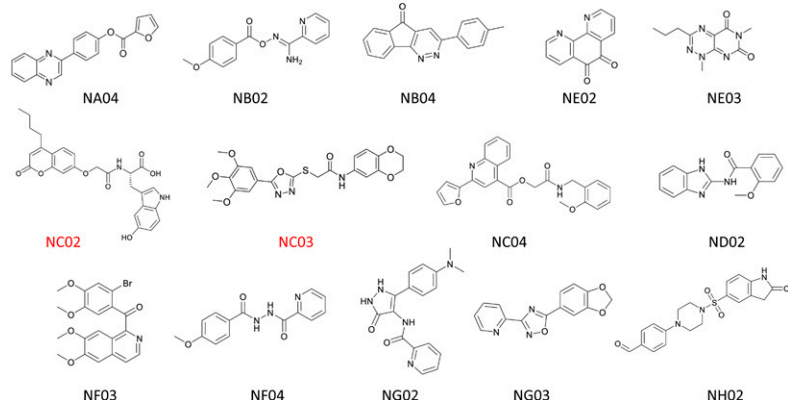


Fig. 3. Chemical structures of the 14 inhibitors identified by these studies.

The precipitated beads capturing the PI4K2A enzyme were tested for kinase activity using the *in vitro* ADP-Glo enzyme assay along with no enzyme or no substrate controls. The results showed a strong correlation between the potency of inhibitors between the enzymes isolated from COS-7 cells and bacteria, indicating that the candidates can inhibit the palmitoylated enzyme in a same manner as well (Fig. 4A, B).

Inhibitory effect of the compounds in *in situ* kinase activity assays

To evaluate the effect of the candidate inhibitors on the enzyme within the cells, *in situ* kinase assays were performed in permeabilized COS-7 cells using radiolabeled γ - 32 P-labeled ATP followed by phosphoinositide extraction, TLC analysis, and quantification. To eliminate the contribution of the activity of PI4KA and PI4KB enzymes that generate a large portion of PI4P within the cells, treatment of the cells with 10 μ M of wortmannin for 10 min was used before treatment with the candidate inhibitors (10 μ M) for 30 min in cell permeabilization buffer to ensure proper penetration of the inhibitors and ATP. Figure 5A shows a representative TLC from one of these experiments and the summary of two experiments is shown in Fig. 5B. This analysis indicated a substantially lower potency of the compounds than what was observed with the isolated proteins and also revealed that some inhibitors also inhibited the labeling of phosphatidic acid, suggesting that they inhibited DG kinase activities. Based on these results, two compounds, code-named NC02 and NC03 (see Fig. 3), were selected for further investigations.

The PI4P pools in Golgi and endosomes decrease upon treatment with NC03

The effects of the two selected inhibitors were then analyzed in live cell confocal imaging of COS-7 cells transfected with GFP-P4M, a reporter showing the different cellular PI4P pools (37). PI4P is produced by different PI4Ks in specific intracellular compartments and, based on previous studies on the localization of the enzyme (6), PI4K2A was expected to be primarily responsible for the endosomal pool and partly responsible for the Golgi pool of PI4P. As shown in Fig. 6, 10 μ M of NC03 elicited a rapid reduction in the Golgi and endosomal PI4P pool. However, NC02 had no noticeable effects (not shown).

Development of a BRET assay to monitor PI4P generation on endosomes

Quantification of the changes in the PI4P level in the endosomes from imaging data is challenging because of

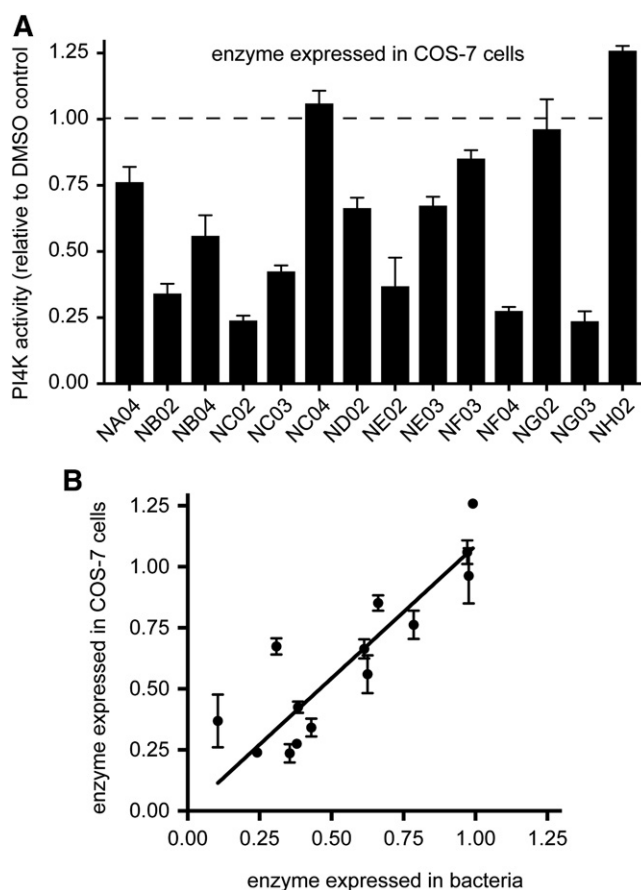


Fig. 4. Effects of PI4K2A inhibitors on PI4K2A expressed in COS-7 cells. A: mRFP-PI4K2A was immunoprecipitated in a two-step pull down from COS-7 cell lysates using anti biotin-conjugated mRFP antibody and streptavidin-coated beads. *In vitro* PI4K2A activity was measured by luminescence-based ADP-Glo™ kinase assay kit, using the human PI4K2A bound to the streptavidin beads. Values were normalized to DMSO-treated controls. Average values and the range of two experiments are shown with each performed in duplicate. B: Correlation between the potencies of PI4K2A inhibitors found in the two assays run either with the enzyme isolated from COS-7 cells or expressed in bacteria. Inhibition was expressed as activity relative to DMSO-treated controls as in panel A.

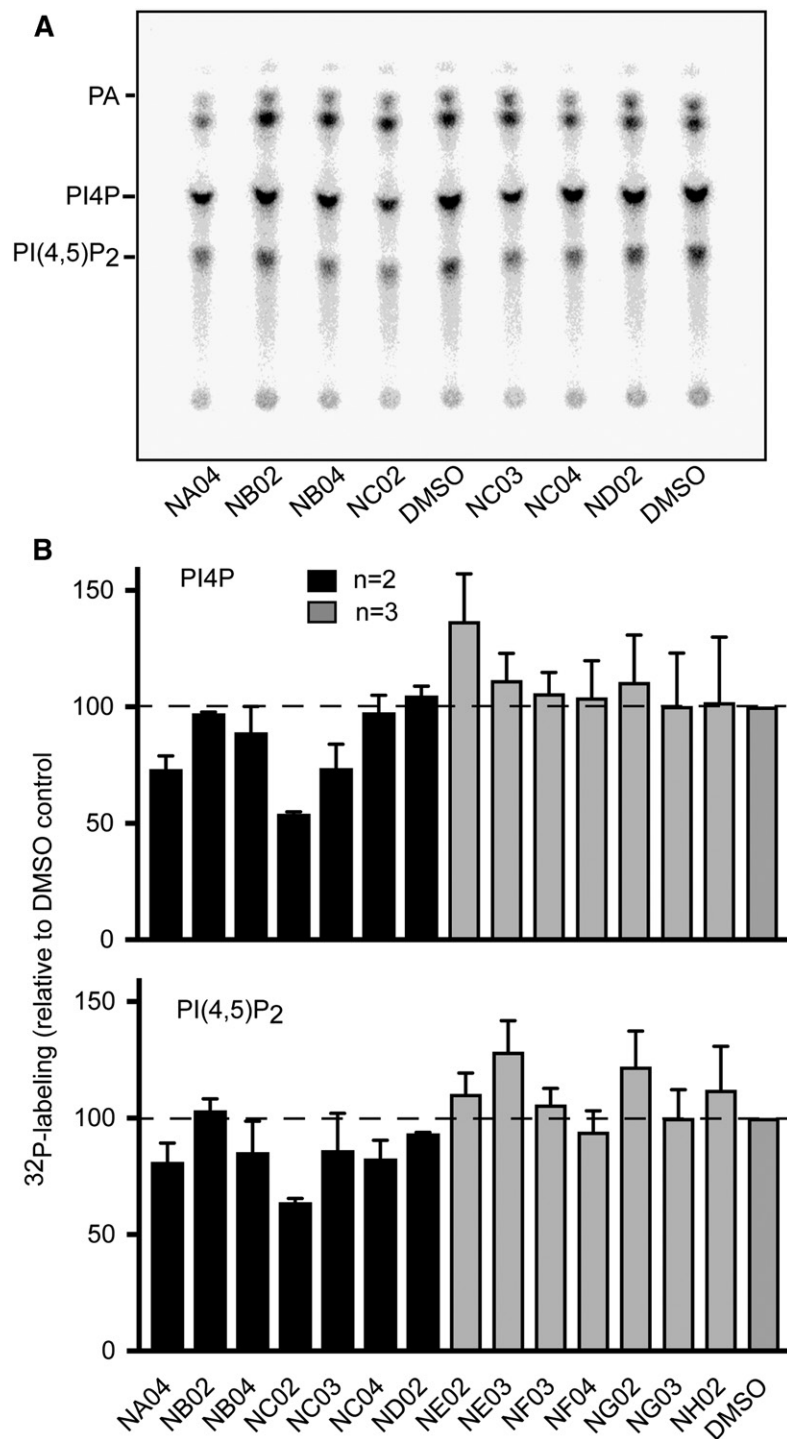


Fig. 5. Effect of the inhibitory compounds on PI4P and PI(4,5)P2 synthesis tested by an in situ kinase assay. A: Picture of the TLC plate from a representative experiment showing the ^{32}P -labeled lipids. COS-7 cells were permeabilized and treated with respective inhibitors prior to adding [^{32}P]ATP. The results show reduction in PI4P and PI(4,5)P2 labeling upon treatment with 10 μM of NC02 or NC03. Note the effect of NA045 on phosphatidic acid (PA) labeling indicating an off-target inhibitory effect on diacylglycerol kinases. B: Quantification of total PI4P and PI(4,5)P2 from three (gray columns) and two (black columns) independent experiments performed in duplicate. Mean values \pm SEM or range are shown.

the heterogeneity of cell expression of the reporter and the requirement for the quantitation from a high number of cells to have a robust signal. This method, therefore, is not practical for the analysis of a high number of compounds for quantitative comparisons. The high content cell imaging assay was used to assess the ability of the compounds to modulate endosomal and Golgi-associated GFP-P4M signals, but it was not robust enough to recognize and quantitate the signals reliably in these compartments. A BRET assay was therefore developed to measure the PI4P pool in the various endosomes in a live cell-based assay to enable the testing of the effects of the compounds and their

dose-dependence for determination of potency and efficacy. Initial BRET measurements were designed to monitor PI4P levels in Rab7-positive late endosomes. For this, we coexpressed the tandem P4M domain of the Legionella SidM protein fused to the Renilla luciferase and the Venus fluorescent protein fused to Rab7. To achieve an equal ratio of coexpression, the luciferase-fused probe and the Rab7-tagged Venus were expressed from a single plasmid separated by the viral T2A peptide sequence. The presence of PI4P in Rab7 endosomes brings the luciferase in proximity to the Venus protein and, in the presence of the coelenterazine substrate, energy-transfer takes place that can be

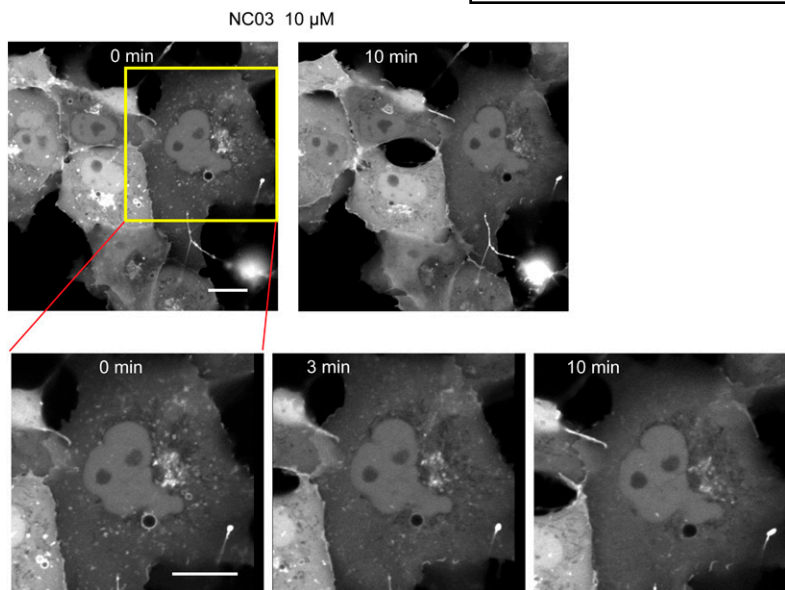


Fig. 6. NC03 treatment affects the intracellular PI4P pools in the Golgi and endosomes. The effect of NC03 on the Golgi and endosomal PI4P pool was investigated by confocal microscopy using the P4M-GFP sensor expressed in COS-7 cells. Cells were transfected with a GFP-tagged P4M for 16–20 h, and cells were imaged live in a Zeiss 710 laser scanning confocal microscope. Addition of NC03 (10 μ M) caused a rapid reduction in the Golgi and endosomal GFP signal over a period of 10 min, indicating a decreased PI4P level in those compartments. One of the cells was enlarged for better details. Bar is 10 μ m.

monitored in a plate reader giving a measurement from whole cell population (46). To increase the availability of the P4M2x-SLuc component in the cytosol, we used an inhibitor of the PI4KA enzyme, which causes elimination of the large PM pool of PI4P, making more of the lipid probe available in the cytosol to find the endosomal PI4P pools (Fig. 7). It is important to note that the PI4KA inhibitor, A1, does not inhibit PI4K2A or PI4K2B (47). Similar experiments performed in identical assays designed for other endosomal pools (namely, Rab4, Rab5, and Rab11) showed very small, if any, PI4P present in those endosomes and

that genetic inactivation of PI4K2A eliminated \sim 80% of the Rab7-associated PI4P assessed by this method (T. Baba et al., unpublished observations). These data have suggested that the BRET assay assessing the Rab7-associated PI4P was a suitable platform to test PI4K2A inhibitors. After verifying the method, all 14 inhibitors were tested using this assay. The results indicated that the NC03 compound decreased PI4P production in the Rab7 compartment by 40–50%. In spite of its potency in the enzyme assays, the NC02 compound failed to show any inhibition in intact cells. This suggested that this compound may have a problem

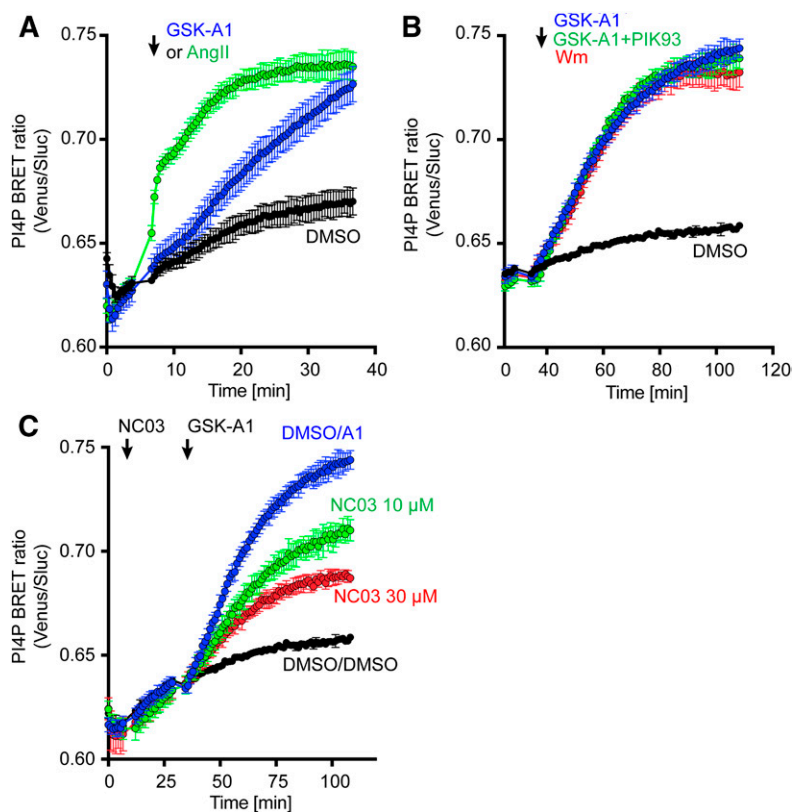


Fig. 7. Quantification of endosomal PI4P changes by BRET analysis upon inhibitor treatment. A live cell-based endosomal BRET assay was developed to measure the PI4P pool specifically in Rab7-positive endosomes, as detailed in the Materials and Methods. HEK-AT1 cells were transfected with Sluc-P4M2X-T2A-Venus-Rab7 construct for 24 h followed by BRET measurement in the presence of the colenterazine substrate (for additional details see the Materials and Methods). The baseline BRET signal measurements were done for 4 min followed by treatment of the cells with various inhibitors as indicated. A: GSK-A1 (10 nM, blue traces), which inhibits PI4KA and therefore reduces PM PI4P levels, or Ang II addition (100 nM, green traces), which activates PLC and rapidly depletes PM PI4P levels, both release the PI4P-sensor, P4M-2x, from the PM and allow its increased association with the endosomal PI4P pool, showing an increased BRET signal with the Rab7-targeted Venus (see the text for more a detailed description of the BRET principle and the components used). B: Similar effects are seen when both the PM and Golgi pools of PI4P were reduced by the less-specific PI4K inhibitor, wortmannin, or with the combination of GSK-A1 (PI4KA inhibitor) and PIK93 (PI4KB inhibitor). C: Increasing concentrations of the NC03 compound reduce the PI4P pool in the Rab7 compartment where PI4K2A is a main source of PI4P. Mean \pm SEM is shown from single experiments, each performed in triplicate. Similar results were obtained in 12 other experiments containing the drugs in other combinations.

entering the cells, an assumption that was tested in further analysis (see below). Several modifications of the original NC03 compound failed to improve its potency or efficacy. The trimethoxy substitution in the bending phenyl ring seemed to be particularly important. All attempts to reduce or change the number of substituents in this ring resulted in a reduction and/or elimination of potency (supplemental Fig. S1). Importantly, there was no structural similarity between PI-273 (35) and any of the active compounds identified in this study.

Modifying NC02 to increase its cell penetration

The NC02 hit consists of three parts: a modified coumarin core, a 5-hydroxytryptophane, and a short acyl linker connecting the two. In the course of the project, the coumarin core was altered ranging from slight modifications (e.g., shortening or elongating its alkyl sidechain) to more substantial modifications, such as introduction of a different heterocycle of similar size (e.g., quinolinone or quinazolinone). The 5-hydroxytryptophane was substituted with other amino acids or their residues (e.g., tyrosine, tryptophane, tryptamine), and the connecting linker was modified in length (one to five atoms) and type of connection at either of the ends (amide, amine, ether, etc.). Over 60 new compounds were prepared; however, none surpassed the parent NC02 compound in biological activity (a selected group is shown in supplemental Fig. S2). Incidentally, during these efforts to improve the lead structure, we prepared a few simple esters (methyl, ethyl, isopropyl) and amides (methyl, dimethyl) of the NC02 hit. Although these compounds proved to possess similar activity in the soluble enzyme assays, due to the lack of the negative charge of the carboxy function, they were found superior in terms of cell penetration (Fig. 8). The preparation of esters was performed very similarly to their original template, only by using different esters of 5-hydroxytryptophane. Amides were prepared by the treatment of a corresponding methylester with methylamine or dimethylamine.

DISCUSSION

This study was aimed at identifying small molecular inhibitors of PI4K2A. The role of this enzyme and its sister enzyme, PI4K2B, in cellular functions is the least understood among the four PI4K enzymes. While most studies found PI4K2A responsible for the majority of the endosomal PI4P pools (48) based on its structural similarities to PI4K2B (19), a functional redundancy between these enzymes likely takes place. A small molecule inhibitor would most probably target both enzymes allowing analysis of their cellular functions under acute inhibition, rather than after their prolonged genetic inactivation.

Our efforts have identified compounds that can be potential starting points for further studies that optimize them. In spite of considerable efforts, we could not modify any of our best hits to increase their potencies and, therefore, we did not pursue further studies at this stage to analyze the specificity of these hits against the larger kinome.

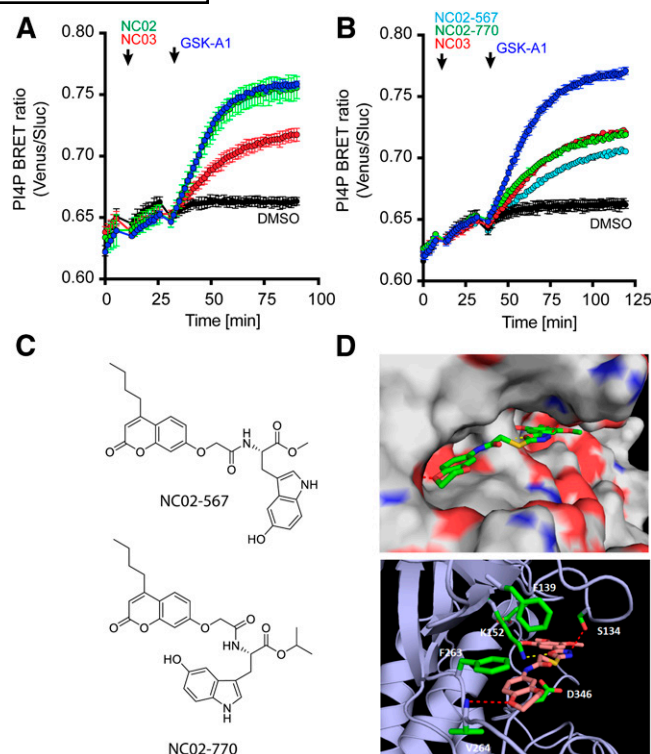


Fig. 8. Modifications in NC02 increased cell penetration resulting in enhancement of the cell potency. BRET analysis was performed as described in the legend to Fig. 7. Following 4 min of the baseline BRET signal measurements, the cells were treated with NC02 or NC03 (10 μ M) (A) or the derivatives NC02-770 and NC02-567 (10 μ M) (B) for 15 min. Cells were then treated with A1 (10 nM) and the BRET signal was measured for 30 min. DMSO was used as a control. Note the lack of effect of NC02 in the cellular assay in spite of its potent inhibitory effect on the enzyme. C: Chemical modifications improved the cell permeability of NC02. Mean \pm SEM is shown from one of two similar experiments performed in triplicate. D: Predicted binding model of NC03 at the active site of PI4K2a. Both the surface representation and the ribbon model are shown. In the ribbon model, the protein is shown in blue, while the key residues interacting with the inhibitor are shown as sticks (green). NC03 bound at the active site is depicted as sticks. Three hydrogen bonds are predicted to be formed with residues S134, F263, and V264 at the active site.

Clearly, these inhibitors are specific among the PI4Ks to the type II isoforms, but they may hit other kinases. For the same reasons, we did not attempt to perform any biological studies until compounds with better potency are found that would be worthy of further analysis. Such efforts are being pursued in our laboratories.

A major advance in this study was the development of a method that allows the analysis of PI4K2A inhibitors in a cellular context using the BRET principle in a plate reader format. This has proven to be an extremely useful tool to test larger numbers of inhibitors without the need of cumbersome lipid analyses. This tool should facilitate testing potential PI4K2A inhibitors in the future. 

The authors are grateful for the DNA constructs provided by the Varnai laboratory (Semmelweis University, Faculty of Medicine, Budapest, Hungary). Confocal imaging was performed at the

Microscopy and Imaging Core of the National Institute of Child Health and Human Development, National Institutes of Health with the kind assistance of Dr. Vincent Schram and Lynne Holtzclaw.

REFERENCES

1. Balla, T. 2013. Phosphoinositides: tiny lipids with giant impact on cell regulation. *Physiol. Rev.* **93**: 1019–1137.
2. Shuttleworth, S. J., F. A. Silva, A. R. Cecil, C. D. Tomassi, T. J. Hill, F. I. Raynaud, P. A. Clarke, and P. Workman. 2011. Progress in the preclinical discovery and clinical development of class I and dual class I/IV phosphoinositide 3-kinase (PI3K) inhibitors. *Curr. Med. Chem.* **18**: 2686–2714.
3. Boura, E., and R. Nencka. 2015. Phosphatidylinositol 4-kinases: function, structure, and inhibition. *Exp. Cell Res.* **337**: 136–145.
4. D'Angelo, G., M. Vicinanza, C. Wilson, and M. A. De Matteis. 2012. Phosphoinositides in Golgi complex function. *Subcell. Biochem.* **59**: 255–270.
5. Nakatsu, F., J. M. Baskin, J. Chung, L. B. Tanner, G. Shui, S. Y. Lee, M. Pirruccello, M. Haio, N. T. Ingolia, M. R. Wenk, et al. 2012. PtdIns4P synthesis by PI4KIIIa at the plasma membrane and its impact on plasma membrane identity. *J. Cell Biol.* **199**: 1003–1016.
6. Minogue, S. 2018. The many roles of type II phosphatidylinositol 4-kinases in membrane trafficking: new tricks for old dogs. *Bioessays.* **40**: doi:10.1002/bies.201700145.
7. Altan-Bonnet, N., and T. Balla. 2012. Phosphatidylinositol 4-kinases: hostages harnessed to build panviral replication platforms. *Trends Biochem. Sci.* **37**: 293–302.
8. Vanhaesebroeck, B., L. Stephens, and P. Hawkins. 2012. PI3K signalling: the path to discovery and understanding. *Nat. Rev. Mol. Cell Biol.* **13**: 195–203.
9. Bianco, A., V. Reghellin, L. Donnici, S. Fenu, R. Alvarez, C. Baruffa, F. Peri, M. Pagani, S. Abrignani, P. Neddermann, et al. 2012. Metabolism of phosphatidylinositol 4-kinase IIIalpha-dependent PI4P is subverted by HCV and is targeted by a 4-anilino quinazoline with antiviral activity. *PLoS Pathog.* **8**: e1002576.
10. Arita, M., H. Kojima, T. Nagano, T. Okabe, T. Wakita, and H. Shimizu. 2011. Phosphatidylinositol 4-kinase III beta is a target of enviroxime-like compounds for antipoliiovirus activity. *J. Virol.* **85**: 2364–2372.
11. Thibaut, H. J., H. M. van der Schaar, K. H. Lanke, E. Verbeke, M. Andrews, P. Leyssen, J. Neyts, and F. J. van Kuppeveld. 2014. Fitness and virulence of a coxsackievirus mutant that can circumnavigate the need for phosphatidylinositol 4-kinase class III beta. *J. Virol.* **88**: 3048–3051.
12. Balla, A., Y. J. Kim, P. Varnai, Z. Szentpetery, Z. Knight, K. M. Shokat, and T. Balla. 2008. Maintenance of hormone-sensitive phosphoinositide pools in the plasma membrane requires phosphatidylinositol 4-kinase III[alpha]. *Mol. Biol. Cell.* **19**: 711–721.
13. Pan, W., S. C. Choi, H. Zhang, Y. Qin, L. Volpicelli-Daley, L. Swan, L. Lucast, C. Khoo, X. Wang, L. Li, et al. 2008. Wnt3a-mediated formation of phosphatidylinositol 4,5-bisphosphate regulates LRP6 phosphorylation. *Science.* **321**: 1350–1353.
14. Qin, Y., L. Li, W. Pan, and D. Wu. 2009. Regulation of phosphatidylinositol kinases and metabolism by Wnt3a and Dvl. *J. Biol. Chem.* **284**: 22544–22548.
15. Tanneberger, K., A. S. Pfister, K. Brauburger, J. Schneikert, M. V. Hadjihannas, V. Kriz, G. Schulte, V. Bryja, and J. Behrens. 2011. Amer1/WTX couples Wnt-induced formation of PtdIns(4,5)P2 to LRP6 phosphorylation. *EMBO J.* **30**: 1433–1443.
16. Jović, M., M. J. Kean, A. Dubankova, E. Boura, A. C. Gingras, J. A. Brill, and T. Balla. 2014. Endosomal sorting of VAMP3 is regulated by PI4K2A. *J. Cell Sci.* **127**: 3745–3756.
17. Jeong, Y. H., M. Sekiya, M. Hirata, M. Ye, A. Yamagishi, S. M. Lee, M. J. Kang, A. Hosoda, T. Fukumura, D. H. Kim, et al. 2010. The low-density lipoprotein receptor-related protein 10 is a negative regulator of the canonical Wnt/beta-catenin signaling pathway. *Biochem. Biophys. Res. Commun.* **392**: 495–499.
18. Bilic, J., Y. L. Huang, G. Davidson, T. Zimmermann, C. M. Cruciat, M. Bienz, and C. Niehrs. 2007. Wnt induces LRP6 signalosomes and promotes dishevelled-dependent LRP6 phosphorylation. *Science.* **316**: 1619–1622.
19. Klima, M., A. Baumlova, D. Chalupska, H. Hrebabecky, M. Dejmeck, R. Nencka, and E. Boura. 2015. The high-resolution crystal structure of phosphatidylinositol 4-kinase IIβ and the crystal structure of phosphatidylinositol 4-kinase IIα containing a nucleoside analogue provide a structural basis for isoform-specific inhibitor design. *Acta Crystallogr. D Biol. Crystallogr.* **71**: 1555–1563.
20. Najdi, R., R. F. Holcombe, and M. L. Waterman. 2011. Wnt signaling and colon carcinogenesis: beyond APC. *J. Carcinog.* **10**: 5.
21. Morris, J. P. t., S. C. Wang, and M. Hebrok. 2010. KRAS, Hedgehog, Wnt and the twisted developmental biology of pancreatic ductal adenocarcinoma. *Nat. Rev. Cancer.* **10**: 683–695.
22. Hezel, A. F., A. C. Kimmelman, B. Z. Stanger, N. Bardeesy, and R. A. Depinho. 2006. Genetics and biology of pancreatic ductal adenocarcinoma. *Genes Dev.* **20**: 1218–1249.
23. Giuliani, N., F. Morandi, S. Tagliaferri, M. Lazzaretti, G. Donofrio, S. Bonomini, R. Sala, M. Mangoni, and V. Rizzoli. 2007. Production of Wnt inhibitors by myeloma cells: potential effects on canonical Wnt pathway in the bone microenvironment. *Cancer Res.* **67**: 7665–7674.
24. Kocemba, K. A., R. W. Groen, H. van Andel, M. J. Kersten, K. Mahtouk, M. Spaargaren, and S. T. Pals. 2012. Transcriptional silencing of the Wnt-antagonist DKK1 by promoter methylation is associated with enhanced Wnt signaling in advanced multiple myeloma. *PLoS One.* **7**: e30359.
25. Huang, S. M., Y. M. Mishina, S. Liu, A. Cheung, F. Stegmeier, G. A. Michaud, O. Charlat, E. Wiellette, Y. Zhang, S. Wiessner, et al. 2009. Tankyrase inhibition stabilizes axin and antagonizes Wnt signalling. *Nature.* **461**: 614–620.
26. Chu, K. M., S. Minogue, J. J. Hsuan, and M. G. Waugh. 2010. Differential effects of the phosphatidylinositol 4-kinases, PI4KIIα and PI4KIIβ, on Akt activation and apoptosis. *Cell Death Dis.* **1**: e106.
27. Walz, H. A., X. Shi, M. Chouinard, C. A. Bue, D. M. Navaroli, A. Hayakawa, Q. L. Zhou, J. Nadler, D. M. Leonard, and S. Corvera. 2010. Isoform-specific regulation of Akt signaling by the endosomal protein WDFY2. *J. Biol. Chem.* **285**: 14101–14108.
28. Schenck, A., L. Goto-Silva, C. Collinet, M. Rhinn, A. Giner, B. Habermann, M. Brand, and M. Zerial. 2008. The endosomal protein App11 mediates Akt substrate specificity and cell survival in vertebrate development. *Cell.* **133**: 486–497.
29. Nazarewicz, R. R., G. Salazar, N. Patrushev, A. San Martin, L. Hilenski, S. Xiong, and R. W. Alexander. 2011. Early endosomal antigen 1 (EEA1) is an obligate scaffold for angiotensin II-induced, PKC-alpha-dependent Akt activation in endosomes. *J. Biol. Chem.* **286**: 2886–2895.
30. Jović, M., M. J. Kean, Z. Szentpetery, G. Polevoy, A. C. Gingras, J. A. Brill, and T. Balla. 2012. Two phosphatidylinositol 4-kinases control lysosomal delivery of the Gaucher disease enzyme, β-glucocerebrosidase. *Mol. Biol. Cell.* **23**: 1533–1545.
31. Gatta, A. T., and T. P. Levine. 2017. Piecing together the patchwork of contact sites. *Trends Cell Biol.* **27**: 214–229.
32. Forrest, S., A. Chai, M. Sanhueza, M. Marescotti, K. Parry, A. Georgiev, V. Sahota, R. Mendez-Castro, and G. Pennetta. 2013. Increased levels of phosphoinositides cause neurodegeneration in a Drosophila model of amyotrophic lateral sclerosis. *Hum. Mol. Genet.* **22**: 2689–2704.
33. Cao, M., Y. Wu, G. Ashrafi, A. J. McCartney, H. Wheeler, E. A. Bushong, D. Boassa, M. H. Ellisman, T. A. Ryan, and P. De Camilli. 2017. Parkinson Sac domain mutation in synaptojanin 1 impairs clathrin uncoating at synapses and triggers dystrophic changes in dopaminergic axons. *Neuron.* **93**: 882–896.e5.
34. Alvarez-Prats, A., I. Bjelobaba, Z. Aldworth, T. Baba, D. Abebe, Y. J. Kim, S. S. Stojilkovic, M. Stopfer, and T. Balla. 2018. Schwann-cell-specific deletion of phosphatidylinositol 4-kinase alpha causes aberrant myelination. *Cell Reports.* **23**: 2881–2890.
35. Li, J., Z. Gao, D. Zhao, L. Zhang, X. Qiao, Y. Zhao, H. Ding, P. Zhang, J. Lu, J. Liu, et al. 2017. PI-273, a substrate-competitive, specific small-molecule inhibitor of PI4KIIalpha, inhibits the growth of breast cancer cells. *Cancer Res.* **77**: 6253–6266.
36. Balla, A., G. Tuymetova, M. Barshishat, M. Geiszt, and T. Balla. 2002. Characterization of type II phosphatidylinositol 4-kinase isoforms reveals association of the enzymes with endosomal vesicular compartments. *J. Biol. Chem.* **277**: 20041–20050.
37. Hammond, G. R., M. P. Machner, and T. Balla. 2014. A novel probe for phosphatidylinositol 4-phosphate reveals multiple pools beyond the Golgi. *J. Cell Biol.* **205**: 113–126.
38. Tóth, J. T., G. Gulyás, D. J. Tóth, A. Balla, G. R. Hammond, L. Hunyady, T. Balla, and P. Várnai. 2016. BRET-monitoring of the

- dynamic changes of inositol lipid pools in living cells reveals a PKC-dependent PtdIns4P increase upon EGF and M3 receptor activation. *Biochim. Biophys. Acta.* **1861**: 177–187.
39. Baumlova, A., D. Chalupska, B. Rozycki, M. Jovic, E. Wisniewski, M. Klima, A. Dubankova, D. P. Kloer, R. Nencka, T. Balla, et al. 2014. The crystal structure of the phosphatidylinositol 4-kinase II α . *EMBO Rep.* **15**: 1085–1092.
40. Nakanishi, S., K. J. Catt, and T. Balla. 1995. A wortmannin-sensitive phosphatidylinositol 4-kinase that regulates hormone-sensitive pools of inositolphospholipids. *Proc. Natl. Acad. Sci. USA.* **92**: 5317–5321.
41. Tai, A. W., N. Bojjireddy, and T. Balla. 2011. A homogeneous and nonisotopic assay for phosphatidylinositol 4-kinases. *Anal. Biochem.* **417**: 97–102.
42. Inglese, J., D. S. Auld, A. Jadhav, R. L. Johnson, A. Simeonov, A. Yasgar, W. Zheng, and C. P. Austin. 2006. Quantitative high-throughput screening: a titration-based approach that efficiently identifies biological activities in large chemical libraries. *Proc. Natl. Acad. Sci. USA.* **103**: 11473–11478.
43. Klima, M., D. J. Toth, R. Hexnerova, A. Baumlova, D. Chalupska, J. Tykvart, L. Rezaczkova, N. Sengupta, P. Man, A. Dubankova, et al. 2016. Structural insights and in vitro reconstitution of membrane targeting and activation of human PI4KB by the ACBD3 protein. *Sci. Rep.* **6**: 23641.
44. Jung, G., J. Wang, P. Wlodarski, B. Barylko, D. D. Binns, H. Shu, H. L. Yin, and J. P. Albanesi. 2008. Molecular determinants of activation and membrane targeting of phosphoinositol 4-kinase IIbeta. *Biochem. J.* **409**: 501–509.
45. Bojjireddy, N., M. L. Guzman-Hernandez, N. R. Reinhard, M. Jovic, and T. Balla. 2015. EFR3s are palmitoylated plasma membrane proteins that control responsiveness to G-protein-coupled receptors. *J. Cell Sci.* **128**: 118–128.
46. Várnai, P., G. Gulyás, D. J. Tóth, M. Sohn, N. Sengupta, and T. Balla. 2017. Quantifying lipid changes in various membrane compartments using lipid binding protein domains. *Cell Calcium.* **64**: 72–82.
47. Bojjireddy, N., J. Botyanszki, G. Hammond, D. Creech, R. Peterson, D. C. Kemp, M. Snead, R. Brown, A. Morrison, S. Wilson, et al. 2014. Pharmacological and genetic targeting of pPI4KA reveals its important role in maintaining plasma membrane PtdIns4p and PtdIns(4,5)p2 levels. *J. Biol. Chem.* **289**: 6120–6132.
48. Dong, R., Y. Saheki, S. Swarup, L. Lucast, J. W. Harper, and P. De Camilli. 2016. Endosome-ER contacts control actin nucleation and retromer function through VAP-dependent regulation of PI4P. *Cell.* **166**: 408–423.